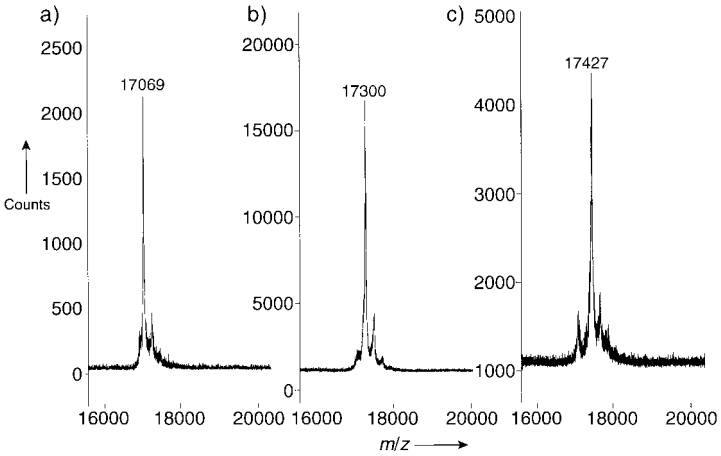

Figure 4. MALDI-TOF spectra of cleaved and labeled GPRT: a) GPRT: expected 17074, observed 17069; b) biotin-labeled GPRT: expected 17300, observed 17300; c) fluorescein-labeled GPRT: expected 17432, observed 17427.

apply to a large number of proteins. Synthesis of water-soluble thioester labels can be accomplished using *tert*-butyl mercaptoacetate, and proteins can be cleaved and labeled with these reagents in a two-step cleavage/labeling reaction under nondenaturing conditions. The affinity-tagged fusion proteins described herein are not significantly different from affinity-tagged fusion proteins produced in expression systems that have already been used to express and purify nearly all of the proteins of yeast for construction of functional protein arrays and microarrays.[24, 25] The combination of those types of expression strategies with removal of the affinity-tag and subsequent labeling with synthetic molecules should prove useful for many in vitro biochemical and proteomic applications. We hope that TEV protease generation of proteins with N-terminal cysteines will be of use in future protein labeling and semi-synthesis applications, and are currently investigating its application to a broader variety of proteins and glycoproteins, including their micro- and nano-fabrication to produce arrays with uniform orientation.

Received: March 1, 2002 [Z18809]

[1] P. E. Dawson, T. W. Muir, I. Clark-Lewis, S. B. H. Kent, *Science* **1994**, *266*, 776.
[2] T. W. Muir, D. Sondhi, P. A. Cole, *Proc. Natl. Acad. Sci. USA* **1998**, *95*, 6705.
[3] T. W. Muir, P. E. Dawson, S. B. H. Kent, *Methods Enzymol.* **1997**, *289*, 266.
[4] T. W. Muir, *Synlett* **2001**, 733.
[5] D. A. Erlanson, M. Chytil, G. L. Verdine, *Chem. Biol.* **1996**, *3*, 981.
[6] T. C. Evans, Jr., J. Benner, M.-Q. Xu, *Protein Sci.* **1998**, *7*, 2256.
[7] T. J. Tolbert, C.-H. Wong, *J. Am. Chem. Soc.* **2000**, *122*, 5421.
[8] L. A. Marcaurelle, L. S. Mizoue, J. Wilken, L. Oldham, S. B. H. Kent, T. M. Handel, C. R. Bertozzi, *Chem. Eur. J.* **2001**, *7*, 1129.
[9] L. Zhang, J. P. Tam, *Anal. Biochem.* **1996**, *233*, 87.
[10] Z. G. Zhao, J. S. Im, K. S. Lam, D. F. Lake, *Bioconjugate Chem.* **1999**, *10*, 424.
[11] M. Villain, J. Vizzavona, K. Rose, *Chem. Biol.* **2001**, *8*, 673.
[12] J. R. Falsey, M. Renil, S. Park, S. Li, K. S. Lam, *Bioconjugate Chem.* **2001**, *12*, 346.
[13] T. C. Evans, Jr., J. Benner, M.-Q. Xu, *J. Biol. Chem.* **1999**, *274*, 3923.
[14] M.-Q. Xu, T. C. Evans, Jr., *Methods (San Diego, CA, US)*, **2001**, *24*, 257.
[15] D. J. Matthews, J. A. Wells, *Science* **1993**, *260*, 1113.
[16] J. L. Harris, B. J. Backes, F. Leonetti, S. Mahrus, J. A. Ellman, C. S. Craik, *Proc. Natl. Acad. Sci. USA* **2000**, *97*, 7754.
[17] W. G. Dougherty, J. C. Carrington, S. M. Cary, T. D. Parks, *EMBO J.* **1988**, *7*, 1281.
[18] W. G. Dougherty, S. M. Cary, T. D. Parks, *Virology* **1989**, *171*, 356.
[19] T. A. Smith, B. D. Kohorn, *Proc. Natl. Acad. Sci. USA* **1991**, *88*, 5159.
[20] L. J. Lucast, R. T. Batey, J. A. Doudna, *BioTechniques* **2001**, *30*, 544.
[21] A.-C. Gavin, M. Bosche, R. Krause, P. Grandi, M. Marzloch, A. Bauer, J. Schultz, J. M. Rick, A.-M. Michon, C.-M. Cruclat, M. Remor, C. Hofert, M. Schelder, M. Brajenovlc, H. Ruffner, A. Merino, K. Klein, M. Hudak, D. Dickson, T. Rudi, V. Gnau, A. Bauch, S. Bastuck, B. Huhse, C. Leutweln, M.-A. Heurtier, R. R. Copley, A. Edelmann, E. Querfurth, V. Rybin, G. Drewes, M. Raida, T. Bouwmeester, P. Bork, B. Seraphin, B. Kuster, G. Neubauer, G. Superti-Furga, *Nature* **2002**, *415*, 141.
[22] K. F. Geoghegan, J. G. Stroh, *Bioconjugate Chem.* **1992**, *3*, 138.
[23] J. C. Carrington, W. G. Dougherty, *Proc. Natl. Acad. Sci. USA* **1988**, *85*, 3391.
[24] M. R. Martzen, S. M. McCraith, S. L. Spinelli, F. M. Torres, S. Fields, E. J. Grayhack, E. M. Phizicky, *Science* **1999**, *286*, 1153.
[25] H. Zhu, M. Bilgin, R. Bangham, D. Hall, A. Casamayor, P. Bertone, N. Lan, R. Jansen, S. Bidlingmaier, T. Houfek, T. Mitchell, P. Miller, R. A. Dean, M. Gerstein, M. Snyder, *Science* **2001**, *293*, 2101.

Icosahedral WAu_{12}: A Predicted Closed-Shell Species, Stabilized by Aurophilic Attraction and Relativity and in Accord with the 18-Electron Rule**

Pekka Pyykkö* and Nino Runeberg

Stable metal clusters are interesting for their own sake and as potential building blocks for nanostructures. This is especially true for gold due to the recently discovered catalytical properties of small or electronically tuned gold clusters.[1, 2] We here predict the existence of a series of isoelectronic clusters that may be particularly stable for three complementary reasons: 1) particularly efficient radial bonding, 2) the aurophilic attraction in the periphery, and 3) relativistic effects:

1) Consider an Au_{12} icosahedron. Its twelve 6s orbitals will span the irreducible representations of point group I_h $a_g + t_{1u} + h_g + t_{2u}$. The first three are spanned by the 6s, 6p, and 5d atomic orbitals of an atom at the center of the icosahedron, respectively. These three levels can hold 18 electrons. This is the number of valence electrons in WAu_{12} or in the isoelectronic ions $[TaAu_{12}]^-$ and $[ReAu_{12}]^+$.
2) As pointed out in ref. [3], covalent bonding and the van der Waals (vdW) bonding behind the metallophilic

[*] Prof. Dr. P. Pyykkö, Dr. N. Runeberg
Department of Chemistry
University of Helsinki
P.O. Box 55 (A.I. Virtasen aukio 1), 00014 Helsinki (Finland)
Fax: (+358) 9-191-50169
E-mail: Pekka.Pyykko@helsinki.fi

[**] This work was supported by The Academy of Finland. The computations were carried out at CSC, Espoo, Finland.

  1433-7851/02/4112-2174 $ 20.00+.50/0

attraction may be comparable in systems such as Au_4^{2+}. It turns out that the optimized peripheral Au–Au distances here are short, about 280 pm. At this distance, two Au^I centers would feel a mutual vdW attraction of roughly up to 100 kJ mol^{-1} per pair,[4] and the icosahedron has 20 such pairs.

3) Both the radial W–Au bonds and the covalent Au–Au bonds among peripheral atoms are substantially strengthened by relativistic effects.[5]

The valence-isoelectronic Au_{13}^{5+} has been discussed earlier at the Extended Hückel level by Mingos.[6] A compound containing this cluster, $[Au_{13}(PMe_2Ph)_{10}Cl_2](PF_6)_3$, was synthesized in 1981.[7] Its icosahedron is comparable with the one studied here, but distorted. Moreover there are earlier calculations on the icosahedral, neutral clusters Au_{13}[8, 9] and $Au_{12}Pd$.[8]

Sun et al. have studied the lighter homologs MCu_{12}[10] and MAg_{12}[11] (M = Sc–Ni,Y–Ag) at the density functional theory (DFT) level with emphasis on magnetic properties and did find maximum stability around M = V or Nb (Group 5). Also the calculated sizes for the systems are comparable with the ones we present here. It must be added that DFT is not reliable for describing the dispersion or vdW part of these bonds.

We have performed ab initio calculations on the neutral icosahedral WAu_{12} cluster and the isoelectronic Ta and Re ions. In order to compare the results for the WAu_{12} cluster with a gold-only case, we have also calculated the Au_{13}^{5+} cluster. It was checked using lower-level calculations (B3LYP/LANL1DZ) that the icosahedral WAu_{12} represents a local minimum; all vibrational frequencies were real and ranged from one of symmetry h at 30 cm^{-1} to one of symmetry t_{1u} at 190 cm^{-1}. This implies thermal excitation of vibrational modes at room temperature, but no danger to the chemical stability. The totally symmetrical Raman-active a_g frequencies are given in Table 2.

Our results are shown in Table 1. The trends in bond length along the isoelectronic series for the central atom M being Ta$^-$, W, Re$^+$, Au^{5+} are given in Table 2 and suggest a minimum near tungsten. The calculated radial W–Au distance of WAu_{12} is about 268 pm at the highest TZVP + P level. It is clearly shorter than the interatomic distance in metallic gold (288 pm). It is also seen that the present isoelectronic species have shorter bonds and larger force constants than the (idealized theoretical or experimental) species Au_{13}^{5+} of Mingos. This suggests that judicious use of tungsten or its neighbors would strongly fortify gold clusters.

Table 1. Calculated distances R [pm] for W–Au and the shortest Au–Au contacts in WAu_{12}.

Method	Basis set	R(W–Au)	R(Au–Au)
RIMP2	TZVP	279.8	294.2
RIMP2	TZVPP	270.2	284.2
SCF	TZVPP	286.8	301.6
RIMP2	TZVPP + f(Au)	268.0	281.7

The role of electron correlation is seen in the comparison between the SCF and RIMP2 level results in Table 2. The W–Au distance is shortened from 287 to 270 or by 17 pm. The concomitant increase of the breathing vibration is from 116 to 147 cm^{-1}. For relativistic effects on gold, see ref. [5].

Table 2. Calculated distances R [pm] for M–Au (M = central atom) and the nearest-neighbor Au–Au contacts, as well as the force constant k [atomic units] and Raman frequency ω_e [cm^{-1}] for the symmetric stretch of the isoelectronic MAu_{12} series (M = Ta$^-$, W, Re$^+$, Au^{5+}). All calculations were done using the TZVPP basis sets.

M	Method	R(M–Au)	R(Au–Au)	k	ω_e
Ta$^-$	SCF	289.1	304.0	1.10	111
W	SCF	286.8	301.5	1.21	116
Re$^+$	SCF	286.2	301.0	1.20	116
Au^{5+}	SCF	309.0	324.9	0.42	69
Ta$^-$	RIMP2	270.4	284.3	1.86	144
W	RIMP2	270.2	284.2	1.93	147
Re$^+$	RIMP2	271.2	285.2	1.69	138
Au^{5+}	RIMP2	279.1[a]	293.4	1.12	112

[a] Experimental distances in $[Au_{13}(PMe_2Ph)_{10}Cl_2](PF_6)_3$ 271.6–278.9 pm.[7]

One possible synthetic route to WAu_{12} could go through atomic vapors of W and Au. Note that W vapor is being used in organometallic synthesis. Another pathway could involve normal chemical reactions of for example WCl_6. In liquid alloys, the binary W–Au phase diagram shows no signs of solubility or stoichiometric compounds.[12] A likely reason is that the W–W bonding is even stronger than the W–Au one. Due to the difficulty of finding thermochemical reference states for W, no stability estimates are given here.

The closed-shell electronic structure and the compact geometry of WAu_{12} should help in isolating it. Its bulk stability could be improved for example by a thiolate or xenon monolayer on the surface. The isoelectronic ions $[TaAu_{12}]^-$ and $[ReAu_{12}]^+$ could form interesting Zintl-type structures including the stoichiometric salt, possibly with covered surfaces.

In the orbital energy spectrum (Figure 1) the positions of the bonding a_g, t_{1u}, and h_g orbitals are of special interest. These three orbitals have to be occupied to fulfil the 18-electron rule. The bonding a_g orbital overlaps with the gold 5d band. The HOMO–LUMO gap is 3.0 eV at the B3LYP/LANL1DZ level. This large gap was already noted for the 3d and 4d analogs by Sun et al.[10] It is interesting that both electron- and hole-type superconductors based on the icosahedral carbon fullerenes have recently been reported.[13] The degenerate h_g symmetric HOMO and LUMO apparently play a role there. The high level of degeneration raises the density of states, which in turn raises the critical temperature. This feature of C_{60} (highly degenerate frontier orbitals) is shared by WAu_{12}. Electrochemically, the h_g HOMO could be oxidized to a maximum loss of ten electrons, and the empty h_g orbital could be reduced to a maximum gain of ten electrons.

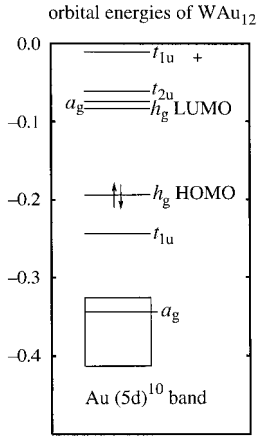

Figure 1. The B3LYP/LANL1DZ orbital energies of WAu_{12} in atomic units.

  1433-7851/02/4112-2175 $ 20.00+.50/0

Finally, just as C_{60} fullerenes yielded fullerene tubes, WAu_{12} could lead to various (now filled) extended structures. Judging from the short W–Au distances, they might have substantial mechanical strength. The mutual coupling of such structures by chemical bonds[14] or by the ionic interactions already mentioned is a further possibility.

Summarizing, if these triply stabilized, icosahedral 5d metal clusters could be made, they might provide a new structural "principle" in gold chemistry.

Computational Methods

The reported calculations have been performed at the Hartree – Fock (HF), second-order Møller – Plesset (MP2), or B3LYP DFT level. The MP2 calculations were performed within the resolution-of-identity (RI) approximation.[15, 16] The core electrons were replaced with quasirelativistic pseudopotentials[17] resulting in 14 and 19 valence electrons for W and Au, respectively. The corresponding valence basis sets are of (7s6p5d)/[6s3p3d] quality and labelled as TZVP. The TZVP was further extended by one f function for both W and Au[18] (TZVPP). The largest basis set, TZVPP + f(Au), was obtained by replacing the single f function in TZVPP by two f functions on gold.[19] All calculations have been done with the TURBOMOLE program package.[20]

Received: December 17, 2001 [Z18400]

[1] D. T. Thompson, *Gold Bull. (London)* **2001**, *34*, 56.
[2] D. A. H. Cunningham, W. Vogel, H. Kageyama, S. Tsubota, M. Haruta, *J. Catal.* **1998**, *177*, 1.
[3] P. Pyykkö, N. Runeberg, *J. Chem. Soc. Chem. Commun.* **1993**, 1812.
[4] P. Pyykkö, T. Tamm, *Organometallics* **1998**, *17*, 4842.
[5] P. Pyykkö, *Chem. Rev.* **1988**, *88*, 563. For the latest benchmarks for relativistic effects on gold atoms, molecules, and solids, see P. Pyykkö, *Angew. Chem.* **2002**, submitted.
[6] D. M. P. Mingos, *J. Chem. Soc. Dalton Trans.* **1976**, 1163. Note that only the bonding orbitals of a_g and t_{1u} symmetry were quoted. The HOMO was wrongly supposed to be t_{1u}. The present bonding h_g orbital was hidden in a 13($5d^{10}$) core band.
[7] C. E. Briant, B. R. C. Theobald, J. W. White, L. K. Bell, D. M. P. Mingos, A. J. Welch, *J. Chem. Soc. Chem. Commun.* **1981**, 201.
[8] R. Arratia-Perez, L. Hernández-Acevedo, *Chem. Phys. Lett.* **1999**, *303*, 641, and references therein.
[9] K. Michaelian, N. Rendón, I. L. Garzón, *Phys. Rev. B* **1999**, *60*, 2000.
[10] Q. Sun, X. G. Gong, Q. Q. Zheng, D. Y. Sun, G. H. Wang, *Phys. Rev. B* **1996**, *54*, 10896.
[11] Q. Sun, Q. Wang, J. Z. Yu, Z. Q. Li, J. T. Wang, Y. Kawazoe, *J. Phys. I* **1997**, *7*, 1233.
[12] A. Prince, G. V. Raynor, D. S. Evans, *Phase Diagrams of Ternary Gold Alloys*, The Institute of Metals, London, **1990**, p. 485.
[13] J. H. Schön, C. Kloc, B. Batlogg, *Nature* **2000**, *408*, 549.
[14] T. F. Fässler, *Angew. Chem.* **2001**, *113*, 4289; *Angew. Chem. Int. Ed.* **2001**, *40*, 4161.
[15] F. Weigend, M. Häser, *Theor. Chem. Acc.* **1997**, *97*, 331.
[16] F. Weigend, M. Häser, H. Patzelt, R. Ahlrichs, *Chem. Phys. Lett.* **1998**, *294*, 143.
[17] D. Andrae, U. Häussermann, M. Dolg, H. Stoll, H. Preuss, *Theor. Chim. Acta* **1990**, *77*, 123.
[18] A. W. Ehlers, M. Böhme, S. Dapprich, A. Gobbi, A. Höllwarth, V. Jonas, K. F. Köhler, R. Stegmann, A. Veldkamp, G. Frenking, *Chem. Phys. Lett.* **1993**, *208*, 111.
[19] P. Pyykkö, N. Runeberg, F. Mendizabal, *Chem. Eur. J.* **1997**, *3*, 1451.
[20] R. Ahlrichs, M. Bär, M. Häser, H. Horn, C. Kölmel, *Chem. Phys. Lett.* **1989**, *162*, 165.

Naked-Eye Sensitive Detection of Immunoglubulin G by Enlargement of Au Nanoparticles In Vitro**

Zhanfang Ma and Sen-Fang Sui*

Methods that enable the rapid, sensitive, accurate, and inexpensive detection of substances in a complex sample matrix are important tools. Immunoassays are based on the use of an antibody that reacts specifically with an antigen to be tested. The quantification of immunoassays is generally achieved by measuring the specific activity of a label, that is, its radioactivity, fluorescence, chemiluminescence, or bioluminescence. Because of its special properties which include ease of preparation, high density, large dielectric constant, and biocompatibility,[1] Au nanoparticles, as an amplification tag, have been the subject of research directed at gene analysis[2] and antibody or antigen detection.[3]

The observation of larger Au nanoparticles is beneficial. However, to increase the labeling efficiency, smaller Au nanoparticles are usually used to prepare the conjugate of the antibody or antigen and colloidal gold.[4] Particularly in histochemistry or cytochemistry, ultra-small Au nanoparticles ($\sim$1.5 nm) are essential.[5]

The sensitivity of the small immunogold particles is usually enhanced by silver staining.[6] While silver enhancement allows the signals from immunogold targeting to be seen on blots, their detecting concentration after silver staining can often reach a level of approximately a picogram per microliter ($pg\,\mu L^{-1}$).[7, 8] This is still much lower than that of fluorescent, radioactive, and enzyme-colorometric methods.[9] The lowest detecting concentration for silver staining is generally acknowledged to be 0.1 $pg\,\mu L^{-1}$.[10]

Herein we use a mixture of $HAuCl_4$ and $NH_2OH \cdot HCl$, instead of silver staining solution, to enlarge immunogold particles immobilized on the nitrocellulose strip, based on the seeding method[11] of detecting human immunoglubulin G (h-IgG) in vitro. Although silver enhancement is commonly used to visualize protein-, antibody-, and DNA-conjugated gold nanoparticles in histochemical electron microscopy studies,[4, 12] it has not been used for the enlargement of Au nanoparticles by $HAuCl_4$ and $NH_2OH \cdot HCl$ in vitro to enhance the detection of h-IgG by the naked eye. The detecting limit of the present method is significantly increased to approximately 10 $pg\,mL^{-1}$, thereby rivaling the limits of fluorescent, radioactive, and enzyme-colorometric methods.[9]

Figure 1 shows the principle behind the method used here. While NH_2OH is thermodynamically capable of reducing Au^{3+} ions to bulk metal,[13] the reaction is dramatically accelerated by Au surfaces.[14] As a result, no new particle

[*] Prof. S.-F. Sui, Dr. Z. Ma
Department of the Biological Sciences & Biotechnology
State-Key Laboratory of Biomembrane
Tsinghua University
Beijing 100084 (P. R. China)
Fax: (+86) 10-6278-4768
E-mail: suisf@mail.tsinghua.edu.cn

[**] This research was financed by grants from the National Natural Science Foundation of China (NSFC) and Tsinghua University.

  1433-7851/02/4112-2176 $ 20.00+.50/0